Eur Biophys J (1987) 14: 307–319

European Biophysics Journal

The superstructure of chromatin and its condensation mechanism

III: Effect of monovalent and divalent cations X-ray solution scattering and hydrodynamic studies

M. H. J. Koch, M. C. Vega, Z. Sayers, and A. M. Michon

European Molecular Biology Laboratory, c/o DESY, Notkestrasse 85, D-2000 Hamburg 52, Federal Republic of Germany

Received May 28, 1986/Accepted in revised form October 2, 1986

Abstract. Solutions of rat liver and chicken erythrocyte chromatin at different ionic strengths were characterized by synchrotron X-ray solution scattering, ultracentrifugation, density and viscosity measurements. Previous observations on nuclei were extended to rat liver, calf thymus and yeast nuclei.

It is shown that with monovalent cations condensation is independent of the nature of the cation whereas with divalent cations there are significant differences related to the preference of base binding over phosphate binding. The consistency of hydrodynamic and scattering results confirm the view that chromatin in solution at low ionic strength has a helix-like superstructure. A survey of X-ray and neutron scattering results in the literature shows that previous interpretations, e.g. in terms of a 10 nm filament, are incompatible with the experimental data at low resolution.

Key words: Chromatin, synchrotron radiation, ultracentrifugation, viscosity, modelling

Introduction

X-ray scattering from chromatin in solution, gels and in nuclei (Perez-Grau et al. 1984; Bordas et al. 1986a, b) led to a model in which chromatin fibres at low ionic strength already possess a helix-like superstructure with a diameter comparable to that of condensed chromatin. The most condensed state is achieved mainly by an almost tenfold reduction of the pitch.

In the present paper we present a further characterization of the chromatin preparations by ultracentrifugation, density and viscosity measurements and examine the consistency of the results with those of X-ray scattering. The effect of progressively increasing ionic strength with monovalent cations, divalent cations and $Co(NH_3)_6^{3+}$ was systematically investigated.

The general nature of the observations on chicken erythrocyte nuclei and chromatin fragments in solution were confirmed by similar experiments on calf thymus, rat liver and yeast nuclei as well as on rat liver chromatin fragments. Further, the sources of discrepancy between the conclusions of previous X-ray and neutron scattering studies and the model proposed earlier by Bordas et al. (1986b) are analysed and it is shown that the earlier interpretations are incompatible with the experimental observation.

Materials and methods

Chromatin fragments from chicken erythrocytes

The methods used for these samples are described by Bordas et al. (1986a). Chromatin concentrations were measured by absorbance at 260 nm and 310 nm in a ZEISS DMR10 spectrophotometer. A concentration of 1 mg chromatin/ml or 0.52 mg DNA/ml corresponds to $A_{260} = 10.4$. Unless otherwise stated all samples (chromatin-EDTA) consisting of fragments with on average 70 to 90 nucleosomes were in TE buffer (5 m*M Tris* HCl, 1 m*M* EDTA, 0.1 m*M* PMSF, pH 7.5).

Condensation of chromatin with monovalent, divalent and trivalent cations

Solutions of chicken erythrocyte chromatin fragments were dialysed against 5 m*M Tris* HCl pH 7.5, 0.1 m*M* PMSF, to eliminate EDTA. The cation concentration of chromatin solutions (3.5 mg DNA/ml) was adjusted by adding small volumes of stock solutions – 500 m*M* for the monovalent and 50 m*M* for the di- and trivalent cations – followed by rapid

vortex mixing. They were kept at 4 °C for at least 1 h before the X-ray measurements. NaCl, KCl, LiCl, CsCl were used in the range 5–70 m*M*; $CaCl_2$, $MgCl_2$, $SrCl_2$, $BaCl_2$, $CdCl_2$, $NiCl_2$, $CoCl_2$, $CuCl_2$ and $MnCl_2$ in the range 0.5–2.2 m*M* and the trivalent complex $Co(NH_3)_6^{3+}$ in the range 0.25 m*M* to 1.1 m*M*.

Partial specific volume of chicken erythrocyte chromatin

The densities of chromatin solutions were determined using a Digital Density Meter DMA 45 with an external measuring oscillator cell DMA 601 M (Anton Paar, Graz), thermostated at 20 °C. CsCl and sucrose solutions of known density (Weast and Astle, 1979) were prepared gravimetrically and were used for calibration. Solutions containing NaCl or $MgCl_2$ were prepared gravimetrically from samples in TE buffer and dry salt to insure proper definition of the partial specific volume (Cohen and Eisenberg 1968).

Analytical ultracentrifugation of chromatin with $MgCl_2$

Measurements were carried out at 20 °C and 25,000 rpm in an MSE CENTRISCAN 75 ultracentrifuge with a standard four place aluminium analytical rotor and single sector cells. Sedimentation coefficients were determined by the moving boundary method with Schlieren optics. The chromatin solutions were dialysed against TE buffer. Samples with $MgCl_2$ were prepared by adding small volumes of 50 m*M* or 100 m*M* $MgCl_2$ stock solutions and mixing with a vortex.

Viscosity measurements

The viscosity of chromatin solutions (0.25–2 mg DNA/ml) in TE buffer was measured using an Ostwald capillary viscometer suspended in a waterbath at 20 °C. The viscometer was cleaned between each use with chromic-sulphuric acid and dried. A volume of 2 ml was used for each measurement and the relative viscosity (η_{rel} = ts/tb) was determined by the flow time taken by the meniscus of the solution (ts) or the buffer (tb) to move from the upper to the lower mark on the viscometer and the specific viscosity ($\eta_{sp} = \eta_{rel} - 1$) was obtained. The shear stress was approximately 5 dyne cm^{-2}. As the densities of the buffers and the solutions differ by less than 0.01% the difference between kinematic and dynamic viscosity was neglected. The values of the intrinsic viscosity were obtained from the slope of plots of η_{sp}/c against the chromatin concentration (c) at a fixed Mg^{++}/bp ratio.

Preparation of nuclei from calf thymus

Thymus glands removed immediately after slaughtering were placed in a solution 0.76% trisodium citrate, 1% D-glucose and 0.2 m*M* PMSF pH 7.4 and transported to the laboratory on ice. Nuclei free from cytoplasmic contaminants, as checked by phase-contrast microscopy (Leitz SM-LUX magnification 200), were obtained by the method of Blodel and Potter (1966) or by that of Jenson et al. (1980).

Preparation of nuclei and chromatin from rat liver

Nuclei were isolated from livers of Wistar rats (less than 6 months old) using, essentially, the method of Hewish and Burgoyne (1973). Livers were homogenised in a Potter-Elvehjem homogeniser with 5 strokes at 300 rpm in 7 ml per g of tissue of a buffer of 0.5 *M* sucrose, 1.8 m*M* $MgCl_2$, 5 m*M* *Tris* HCl, 25 m*M* KCl, 0.14 m*M* spermidine, 2 m*M* EGTA and 0.5 m*M* PMSF pH 7.5. The homogenate was centrifuged at 800 g for 10 min. The resulting pellet was homogenised in 7 volumes of the previous buffer with 2.2 *M* sucrose, layered over an equal volume of the same buffer and centrifuged at 76,000 *g* for 45 min. The nuclear pellet was washed twice in a buffer of 5 m*M* *Tris* HCl, 25 m*M* KCl, 25 m*M* NaCl, 1.8 m*M* $MgCl_2$, 0.14 m*M* spermidine and 0.5 m*M* PMSF pH 7.5. Digestion was carried out in 2 different buffers, one containing 150 m*M* NaCl, 0.5 m*M* $CaCl_2$, 10 m*M* *Tris* HCl and 0.5 m*M* PMSF at pH 7.5 and the other containing 25 m*M* KCl, 25 m*M* NaCl, 0.14 m*M* spermidine, 10 m*M* *Tris* HCl, 3 m*M* $MgCl_2$, 0.5 m*M* $CaCl_2$ and 0.5 m*M* PMSF at pH 7.5. Nuclei at 5 mg DNA/ml were digested at 37 °C with 15 Boehringer U/mg DNA of Micrococcal Nuclease (Sigma) for 30 s in the first buffer and with 12.5 U/mg DNA for 45 s in the second buffer. After centrifugation at 800 *g* for 5 min, the pellet was resuspended in the digestion buffer without $CaCl_2$ and supplemented with 1 m*M* EDTA. Centrifugation under the same conditions yields a pellet containing the longer fragments of chromatin which were solubilized in a buffer containing 1 m*M* EDTA, 5 m*M* *Tris* HCl, 0.5 m*M* PMSF at pH 7.5. The supernatant obtained by centrifugation at 20,000 *g* for 15 min was dialysed against the same extraction buffer.

Samples of nuclei and long chromatin fragments were taken for histone and DNA characterization. Histones were extracted by the method of Johns et al. (1960) and 15% polyacrylamide gels were run under the conditions given by Laemmli (1970). The result of this analysis are illustrated in Fig. 1.

The size disribution of the DNA extracted by the method of Axel et al. (1974) was obtained from 1.5% agarose gels in *Tris* acetate buffer run for 5 h at 100 V and stained for 1 h in the dark with Ethidium bromide at a concentration of 1 μg/ml in the same buffer. The gels were photographed using a transilluminator (C61, UV products) on Polaroid type 665 film.

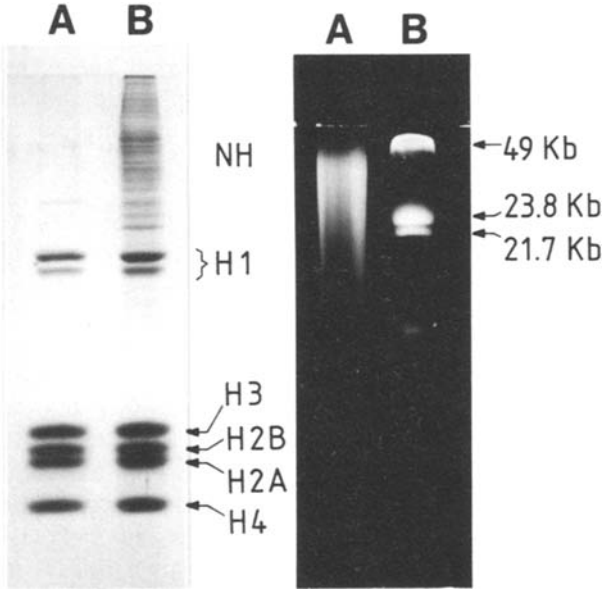

Fig. 1. *Left panel:* SDS polyacrylamide (15%) gel of the histone complement of native rat liver chromatin (*A*) and nuclei (*B*). *Right panel:* Agarose (1.5%) gel of DNA *A*: rat liver chromatin fragments; *B*: mixture of λ phage DNA and ECO RI and Hind III restriction fragments

Preparation of yeast nuclei

Yeast, strain DBY874, were grown over 18–20 h to the early logarithmic phase in a medium of 1% Gibco yeast extract, 2% gelatine hydrolysate peptone No. 190 (Gibco) and 2% D-glucose at 30 °C. Nuclei were prepared from 800 ml of culture following the principle of the method of Rozijn and Tonino (1964). Protoplasts were prepared by digestion at 30 °C for approximately 1 h with 2% β-Glucuronidase (Sigma) and 2.25 mg/ml Zymolase 20T (Miles) in a buffer of 20 m*M* potassium phosphate pH 6.5, 0.75 m*M* $MgCl_2$ with 0.5% β-mercaptoethanol and 1.1 *M* sorbitol. To release the nuclei, protoplasts were lysed and homogenised at 4 °C in 0.02% Triton X-100 (Bio-Rad) in 8% PVP 40,000, 0.75 m*M* $MgCl_2$, 20 m*M* Potassium phosphate pH 6.5 and 0.5 m*M* PMSF (PVP medium). Nuclei and some cytoplasmic components were collected by centrifugation at 21,000 *g* for 30 min at 4 °C and resuspended in 0.6 *M* sucrose in PVP medium. Separation of nuclei was achieved using the sucrose gradient described by Rozijn and Tonino (1964).

Results

Partial specific volume of chicken erythrocyte chromatin

The values of the partial specific volume ($\bar{v}$) of chicken erythrocyte chromatin at different ionic strengths given in Table 1 were obtained from the average of the values of $\bar{v} = 1/\varrho_0 (1 - \Delta\varrho/c)$ for every chromatin concentration (c). ϱ_0 is the density of the buffer or salt solution, $\Delta\varrho$ the difference between the values of the density of the solution and that of the pure buffer or salt solution. The elemental composition, molecular weight (MW = 293,910) and number of electrons (Ne = 156,194) of

Table 1. Density of CE chromatin at different concentrations and ionic strengths and corresponding partial specific volumes

		Density [g/cm³]			
Chromatin concentration [mg/ml]	No salt	1.5 m*M* $MgCl_2$	3 m*M* $MgCl_2$	50 m*M* NaCl	80 m*M* NaCl
0	0.9986	0.9986	0.9987	1.0006	1.0018
4.03	1.0000	1.0000	1.0002	1.0020	1.0032
5.46	1.0005	1.0005	1.0006	1.0024	1.0037
6.41	1.0008	1.0008	1.0009	1.0027	1.0040
7.21	1.0011	1.0011	1.0012	1.0030	1.0043
8.40	1.0015	–	–	–	–
8.84	1.0016	–	–	–	–
Partial specific volume [cm³/g]					
	0.659 ± 0.001	0.654 ± 0.001	0.651 ± 0.002	0.665 ± 0.01	0.653 ± 0.02

the nucleosome including the linker DNA (50 bp) were calculated from the amino acid sequences of histones given by Fasman (1976) for core histones and by Aviles et al. (1978) for the H5 histone. For the 39,141 atoms the percentage composition is C 24.64%, H 49.95%, O 15.57%, N 8.66%, S 0.03%, P 1.07%. From the partial specific volume $\bar{v} = 0.659$ cm^3/g of chromatin, its molecular weight (M) and Avogadro's number (N), a volume $V = \bar{v} N/M = 321.7$ nm^3 is obtained for the nucleosome corresponding to an electron density in pure water of 484.0 e/nm^3 in agreement with the values quoted by Sperling and Tardieu (1976). Taking the electron density of water to be 330 e/nm^3, the excess scattering mass of the nucleosome including Hl is about $4 \cdot 10^4$ electrons against about $7 \cdot 10^3$ for the linker DNA. At very low angles the features of the scattering pattern will thus be dominated by the contribution of the nucleosomes.

Characterization of the X-ray scattering patterns from rat liver and calf thymus nuclei at high and low ionic strength

Features very similar to the ones described for chicken erythrocyte nuclei (Bordas et al. 1986a) are also observed for pellets of rat liver and calf thymus nuclei as illustrated in Fig. 2. For the latter samples, the scattering data were only collected in the range $0.025 < s < 0.18$ nm^{-1}. At high ionic strength (calf thymus nuclei – 150 mM NaCl (A), rat liver nuclei – 100 mM NaCl (B)) there is a weak band at 0.045 nm^{-1}, a band at 0.083 nm^{-1} and a prominent band near 0.15 nm^{-1} as well as a trough near 0.22 nm^{-1} and bands near 0.275 and 0.36 nm^{-1}. Both patterns also display a band at very low angles ($s < 0.025$ nm^{-1}) which is absent in the corresponding solution patterns. This band has been observed in several types of nuclei and attributed to the side by side packing of chromatin fibres (Baudy and Bram 1979; Langmore and Schutt 1980; Langmore and Paulson 1983; Bordas et al. 1986a; Williams et al. 1986; Notbohm 1986a).

The features of the pattern at low ionic strength of rat liver nuclei (C) and of calf thymus nuclei (D) are: a broad strong band at 0.06 nm^{-1} and a band near 0.156 nm^{-1}, a trough near 0.22 nm^{-1} and bands near 0.275 and 0.36 nm^{-1}.

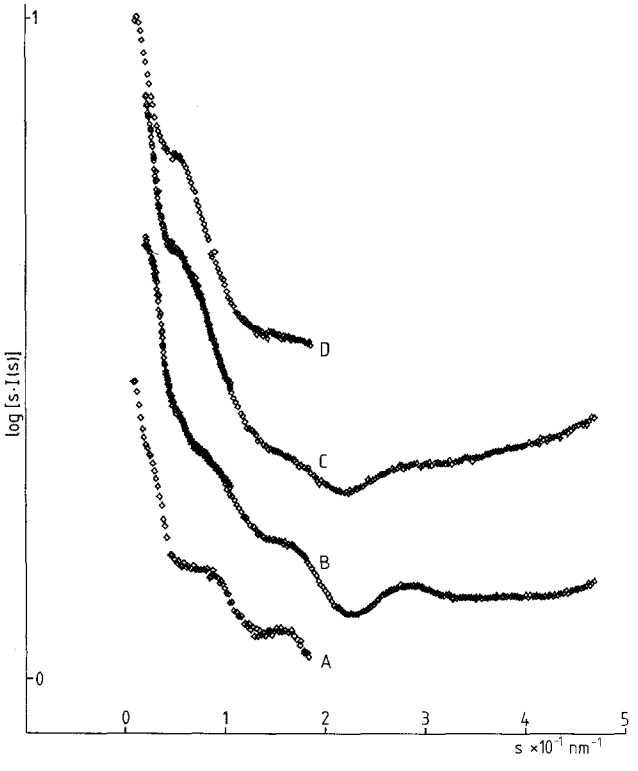

Fig. 2. X-ray scattering patterns from pellets of calf thymus nuclei: $A = 150$ mM NaCl, $D = 1$ mM EDTA and rat liver nuclei $B = 100$ mM NaCl, $C = 1$ mM EDTA displayed as plots of log ($s\,I(s)$) vs. s

Characterization of the low angle scattering pattern of yeast nuclei

The patterns from whole yeast and from nuclei obtained from the 2 M fraction of the sucrose gradient are illustrated in Fig. 3 together with a pattern from rat liver nuclei in 150 mM NaCl. Patterns from nuclei as well as from whole yeast display a strong interference band. The centre of the band appears at about 0.035 nm^{-1} in 20 mM Potassium phosphate and shifts to values close to 0.04 nm^{-1} in 4 mM $MgCl_2$. Simultaneously, its intensity becomes weaker as expected from a decreasing interfibrillar distance (Oster and Riley 1952). The position of the interference band sets a lower limit to the centre-to-centre separation between fibres at about 25 nm as opposed to 35–40 nm in chicken erythrocyte, calf thymus and rat liver chromatin. There is also a broad band at 0.075–0.080 nm^{-1}.

Assignment of the bands to contributions from chromatin was verified by digestion with Micrococcal Nuclease or with DNAse I.

Mass per unit length

The mass per unit length of chicken erythrocyte chromatin-EDTA was determined relative to F-actin in a manner similar to that used by Greulich et al. (1986). Taking the data used for the determination of the partial specific volume and a mass per unit

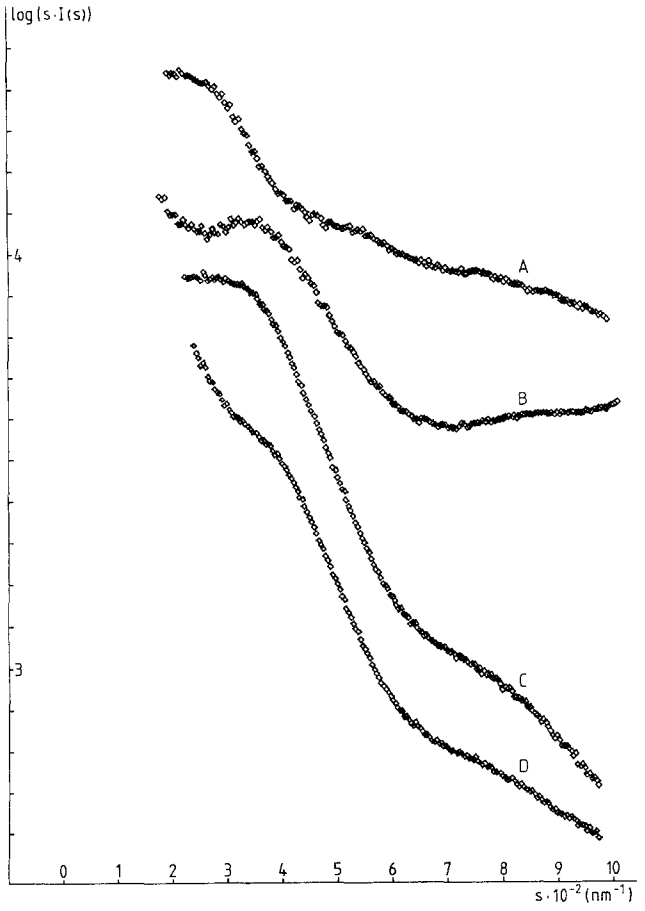

Fig. 3. Low angle scattering pattern of rat liver nuclei (*A*), whole yeast (*B*) yeast nuclei in phosphate buffer (*C*) and in 4 m*M* $MgCl_2$

length of 15,500 Daltons/nm for F-actin (Elzinga et al. 1973) a value of 21.6 ± 2.0 10^3 Daltons/nm or 0.8 ± 0.1 nucleosomes/11 nm is obtained. Since, as observed by Bordas et al. (1986a) and shown below, condensation is accompanied by an eightfold increase of the mass per unit length the condensed 30 nm fibre must have 6.4 ± 0.8 nucleosomes/11 nm in agreement with other observations (Thoma et al. 1979).

Native chromatin fragments in solutions of different ionic strength

Monovalent cations

Rat liver chromatin. The scattering pattern of a solution (4.2 mg DNA/ml) of long chromatin fragments (120 nucleosomes) at low ionic strength is illustrated in Fig. 4. It presents all the characteristic features previously found in chicken erythrocyte preparations (Bordas et al. 1986a), i.e. a band at 0.05 nm^{-1},

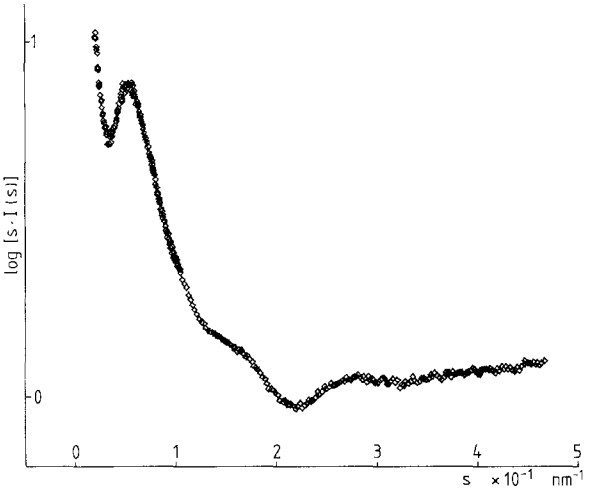

Fig. 4. Solution scattering pattern of rat liver chromatin at low ionic strength (0.2 m*M* EDTA)

a band at 0.145 nm^{-1}, a trough at 0.22 nm^{-1} and a band at 0.275 nm^{-1}.

Upon addition of salt, the same effects as in chicken erythrocyte chromatin are observed as illustrated in Fig. 5, although it appears that rat liver chromatin condenses at lower cation/bp ratios. The corresponding pattern from chicken erythrocyte chromatin fragments (70–90 nucleosomes) at low ionic strength is also shown for comparison. The maximum of the 0.050 nm^{-1} band appears to be shifted to higher *s*-values near 0.055 nm^{-1} and to be slightly more pronounced in the pattern from rat liver chromatin. The changes in the radius of gyration of the cross-section and in the relative mass per unit length also given in Fig. 5 follow the same trends as previously observed for chicken erythrocyte preparations. Note that the values of the radius of gyration of the cross-section are lower than for chicken erythrocyte chromatin, about 7.5 nm at low ionic strength against about 9.5 nm for chicken erythrocyte chromatin.

Chicken erythrocyte chromatin. The values of the radius of gyration of the cross-section and of the relative mass per unit length for the alkali chlorides follow the same trends as previously reported for chicken erythrocyte chromatin in the presence of NaCl (Bordas et al. 1986a). At the chromatin concentrations used (3.5 mg DNA/ml) no precipitation was detected below 80–100 m*M* salt concentration, independent of the nature of the cation.

Divalent and trivalent cations

A systematic study of the behaviour of chromatin in the presence of divalent cations and in absence of EDTA, to avoid competitive binding, gives very

Table 2. Values of $I(0)$ and radius of gyration of the cross-section Rx (in nm) obtained from $\log(s\,I(s))$ vs. s^2 plots for CE chromatin fragments (3.5 mg DNA/ml) as a function of salt concentration for divalent metal chloride solutions. The values of $I(0)$ are on an arbitrary scale but consistent for all series

Concentration [mM]	$MgCl_2$		$CaCl_2$		$SrCl_2$		$BaCl_2$	
	$I(0)$	Rx	$I(0)$	Rx	$I(0)$	Rx	$I(0)$	Rx
0	10.0	9.1	10.0	9.1	10.0	9.3	10.0	9.2
0.50	12.8	9.3	12.5	9.1	15.5	10.6	15.7	9.3
1.00	16.9	9.5	14.1	7.3	18.3	9.9	18.7	9.1
1.25	19.4	9.2	17.0	6.8	21.7	9.7	22.7	9.0
1.50	23.7	8.9	22.2	6.3	26.5	9.4	30.1	8.9
1.75	29.8	8.7	30.6	6.7	32.9	9.2	38.1	8.6
2.00	37.0	8.5	42.1	7.3	41.1	8.7	48.9	8.4
2.20	47.5	8.7	54.3	8.1	53.7	8.9	62.7	8.7

Concentration [mM]	$MnCl_2$		$CoCl_2$		$NiCl_2$		$CuCl_2$		$CdCl_2$	
	$I(0)$	Rx	$I(0)$	Rx	$I(0)$	Rx	$I(0)$	Rx	$I(0)$	Rx
0	10.0	9.1			10.0	9.2	10.0	9.3	10.0	8.6
0.5	13.3	9.3			12.1	9.4	11.6	9.3	10.4	8.4
0.7			9.3	9.7						
1.0	18.4	9.7			15.6	9.2	14.5	9.2	14.9	8.7
1.25	20.2	9.7			19.4		19.3	9.0	17.8	8.5
1.4			12.2	9.0			20.3	8.7		
1.5	29.8	9.0			23.8	8.7	25.4	8.3	23.1	8.1
1.6							30.3	8.3		
1.75	35.5	8.9	19.4	8.7	30.4	8.6	37.9	8.2	30.5	8.0
1.93			28.7	8.6						
2.0	50.6	9.1			40.8	8.5	57.6	9.2	38.7	8.1
2.07			37.5	8.6						
2.2	74.0	9.3	44.4	8.6	57.6	9.0	95.5	11.6	52.3	8.4
2.41			59.1	9.0						
2.76			82.0	10.4						
3.1			127.0	12.7						

similar results to those described earlier (Bordas et al. 1986a) for $MgCl_2$. In particular, the values of the radius of gyration of the cross-section, given in Table 2 together with the corresponding values of $I(0)$, present a minimum at increasing ionic strength, before precipitation occurs. The salt concentration at which this minimum occurs depends on the nature of the cation.

Viscosity and sedimentation measurements

The values of the specific viscosity at different chromatin concentration and fixed Mg^{++}/bp ratio are given in Table 3 together with the corresponding values of the intrinsic viscosity $[\eta]$. There is a linear relationship between $[\eta]$ and the chromatin concentration at a fixed Mg^{++}/bp ratio as well as between η_{sp} and the Mg^{++}/bp ratio at a fixed chromatin concentration.

The dependence of the sedimentation coefficient on chromatin concentration for fractions with an average fibre length of 55 and 90 nucleosomes at different $MgCl_2$ concentrations are given in Table 4. The values of S_0/S as a function of chromatin concentration at fixed Mg^{++}/bp ratio were fitted to an equation of the form $S = S_0(1 + k\,c)^{-1}$ (see for instance Cantor and Schimmel 1980). The slope of the least squares line passing through one at the origin in the plot of S_0/S vs. chromatin concentration yields values of $k = 113$ ml/g for chromatin (90 nucleosomes) at low ionic strength and $k = 75$ ml/g at a Mg^{++}/bp ratio of 0.13. In an ideal system $k = [\eta]$, in very good agreement with the direct viscosity measurements.

Discussion

Several models essentially founded on different types of helical structures have been proposed for chromatin on the basis of electron microscopy and X-ray scattering: solenoid (Finch and Klug 1976), twisted ribbon (Worcel et al. 1981; Woodcock et al. 1984), superbeads (Renz et al. 1977; Stratling et al. 1978) and related layered structures (Subirana et al.

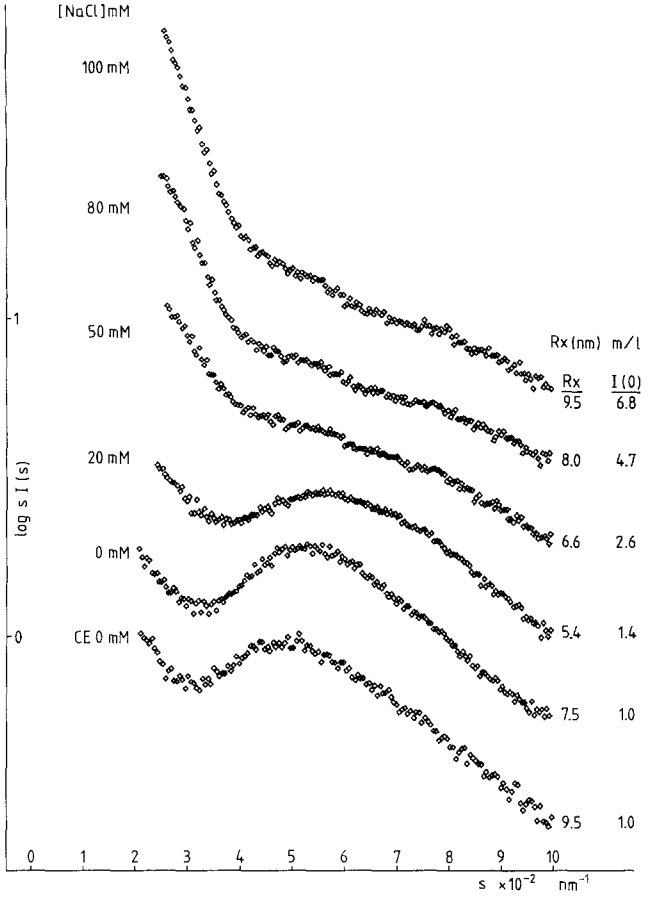

Fig. 5. Changes in the low angle solution scattering pattern of rat liver chromatin (3.5 mg DNA/ml) as a function of NaCl concentration. The bottom curve is the pattern of a similar CE chromatin solution

1985) and finally crossed linker models (Bordas et al. 1986b; Williams et al. 1986). An obvious requirement for any model should be to explain not only the variety of structures which are observed under different ionic conditions, but also to provide a basis for a mechanism by which rapid reversible transitions between different states can occur. These rapid transitions ($t < 50$ ms) have been detected by X-ray (Bordas et al. 1986a) and optical salt jump experiments (Girardet and Roche 1985). At this stage it is thus important to find experimental criteria allowing to exclude, if possible, certain classes of models and/or to characterize more precisely the conditions under which the various structures exist.

Linker length and fibre diameter

Crossed linker models predict the existence of a relationship between linker length and fibre diameter whereas solenoids have fewer constraints in this respect.

Table 3. Experimental values of $\eta_{sp/c}$ and of the intrinsic viscosity $[\eta]$ at different chromatin concentration and fixed Mg^{++}/bp ratio

Chromatin [mg/ml]	$\eta_{sp/c}$ [ml/g]	
Mg^{++}/bp = 0.0		$[\eta] = 113$ ml/g
0.513	119.0	
1.060	120.8	
2.043	136.5	
2.933	139.4	
Mg^{++}/bp = 0.13		$[\eta] = 76$ ml/g
0.444	76.6	
0.906	79.4	
2.112	80.5	
Mg^{++}/bp = 0.30		$[\eta] = 42$ ml/g
0.451	37.7	
0.960	45.8	
2.016	39.7	
2.104	46.6	
2.918	39.1	
Mg^{++}/bp = 0.50		$[\eta] = 33$ ml/g
0.468	32.0	
0.889	30.4	
1.776	27.6	
2.304	26.9	

Table 4. Sedimentation coefficient (Svedberg) of chromatin fragments at different $MgCl_2$ concentrations. The values at infinite dilution were obtained by linear extrapolation for sample I and by parabolic fit for sample II

Sample I: Average length 55 nucleosomes

$MgCl_2$ [m*M*]	Chromatin [mg/ml]		
	0.0	1.5	3.0
0.0	44.5	34.6	24.4
0.2	47.0	36.7	25.6
0.4	38.5	32.4	25.4
0.6	64.0	44.8	26.7
0.8	75.0	50.5	26.6
1.0	83.0	58.5	33.7

Sample II: Average length 90 nucleosomes

$MgCl_2$ [m*M*]	Chromatin [mg/ml]				
	0.0	1.2	2.5	6.0	12.0
0.0	58.0	50.0	45.0	27.5	15.0
0.5		50.0	45.0		
1.0	80.0	65.0	60.0	30.0	17.0
1.5	108.0	90.0	75.0	42.5	32.0
2.0				60.0	48.0
2.5				110.0	70.0

Williams et al. (1986) have recently reported such a relationship based on the assignment of the band near 0.045 nm^{-1} in the scattering pattern of nuclei from species presenting a wide range of linker length to the second maximum of the transform of the equivalent cylinder. The value of the fibre diameter of chicken erythrocyte chromatin given by these authors is 31.9 nm. Bordas et al. (1986b) give a value of 38 nm for the diameter of the equivalent solid cylinder based on the radius of gyration of the cross-section and on the position of the 0.045 nm^{-1} band in the solution scattering pattern of condensed chromatin.

Indirect evidence about the fibre diameter can also be obtained from the position of the interference band near $s = 0.025\ nm^{-1}$ in the scattering patterns from nuclei, illustrated in Fig. 2. This band results from the lateral packing of chromatin fibres (Baudy and Bram 1979; Langmore and Paulson 1983; Bordas et al. 1986a) and is also observed in gels (Bordas et al. 1986a) and appears as a strong equatorial band in the patterns of oriented chromatin samples (Widom and Klug 1985).

Williams et al. (1986) only observe this band in chicken erythrocyte nuclei using a buffer containing, among other things, 60 m*M* KCl, 15 m*M* NaCl and 3 m*M* $MgCl_2$ but not if $MgCl_2$ was replaced by EDTA. With chicken erythrocyte nuclei, Bordas et al. (1986a) observed the band in lysed nuclei in the absence of salt and in intact nuclei in a buffer containing 150 m*M* NaCl, but not in a buffer with 10 m*M* NaCl and 3 m*M* $MgCl_2$. The difference between the observations probably results, as foreseen by the theory of Manning (1978), from the increased threshold for precipitation or condensation by $MgCl_2$ due to higher concentrations of monovalent cations (Borochov et al. 1984). As illustrated in Fig. 2 we observe this band in calf thymus and rat liver nuclei above 100 m*M* NaCl, but the data for lysed nucei – EDTA do not extend to sufficiently small angles to obtain a definite indication.

The spacing of the band is variable in different types of nuclei, ranging from $(40\ nm)^{-1}$ in chicken erythrocyte nuclei to $(32\ nm)^{-1}$ in mouse lymphocyte nuclei (Langmore and Paulson 1983).

The interference band occurs at *s*-values determined by the inverse of the centre-to-centre separation between the fibres (a) (Oster and Riley 1952) and can thus obviously not occur at spacings smaller than that of the 10 reflexion of the corresponding unbounded hexagonal lattice, i.e. a $\sqrt{3}/2$. Its exact position and intensity depend on the ratio $\gamma = a/D$, where D is the diameter of the fibres. Model calculations indicate that in the case of packing of ideal cylinders with 38 nm diameter, the interference band would not occur above 0.028 nm^{-1} in a $\log(s\,I(s))$ vs. s plot, whereas the upper limit for hexagonal packing would be 0.0304 nm^{-1}. Bands in the range 0.023–0.025 nm^{-1}, as observed, are consistent with a fibre diameter of 38 nm and a value of γ of 1.05–1.15.

If the fibre diameter is 31.9 nm, the maximum of the cylinder transform occurs at about 0.052 nm^{-1} and the maximum spacing for the interference band would be 0.0325 if $\gamma = 1$. In this case, however, there would be no contrast between the fibres and the band would be too weak to be detected. Spacings above 0.030 nm^{-1} as observed by Langmore and Paulson (1983) in mouse lymphocyte nuclei ($1/32 = 0.0312\ nm^{-1}$) can thus be taken as an indication of a reduced fibre diameter.

Although a range of linker lengths is compatible with crossed linker or solenoid models it is not entirely clear how this would apply in the case of chromatins with very short repeats (165 bp), e.g. cerebral cortex neurons (Pearson et al. 1983) or yeast (Thomas and Furber 1976). In the latter case the linker length is variable (Rattner et al. 1982). Our results on yeast nuclei indicate that the diameter of the fibre does not exceed 20–25 nm, in agreement with the electron microscopic observations of Rattner et al. (1982) who reported a diameter of 20–30 nm for the higher order fibres in yeast. One may speculate that the apparent absence of H1 in yeast (Brandt et al. 1980) is related to the reduced conformational flexibility resulting from the short linker eliminating the need for the additional constraint.

The absence of the interfibrillar interference band can be interpreted as resulting from a larger centre-to-centre distance between fibres (i.e. a larger value of γ) which would move it to smaller *s*-values outside the range of observation. Langmore and Paulson (1983) observed a shift from 0.025 nm^{-1} to 0.0182 nm^{-2} at low ionic strength, as expected from the increased repulsion between fibres under those conditions. Similar observations were made by Notbohm (1986a). At higher degrees of fibre packing the interference band moves to higher *s*-values, but becomes very weak as in yeast nuclei or disappears because of the loss of contrast between fibres. This could be the case when condensation is induced by divalent cations (Bordas et al. 1986a; Widom et al. 1985).

Widom et al. (1985) concluded on the basis of an electron microscopic and X-ray study of a long repeat (240 bp) chromatin that the diameter of the fibre is independent of the linker length. Unfortunately, since the published micrographs do not provide an unequivocal size comparison and the X-ray data do not extend below $s = 0.03\ nm^{-1}$, these results cannot be taken as definitive proof.

Evidence for a dependence of the fibre radius on the linker length can also be obtained from X-ray solution scattering. If one assumes that the linker DNA is straight at very low ionic strength, a reduction in linker length is expected to result in a smaller radius of gyration of the cross-section and in a shift of the 0.05 nm^{-1} band to larger s-values. The lower values of the radius of gyration of the cross-section in the low ionic strength pattern of rat liver chromatin as compared to chicken erythrocyte chromatin are consistent with a shorter linker in rat liver (35 bp) than in chicken erythrocyte chromatin (50 bp). In the absence of salt, there is also a slight shift of the 0.05 nm^{-1} band to higher angles than in chicken erythrocyte chromatin as illustrated in Fig. 5.

In this context it is important to note that the 0.05 nm^{-1} band in the pattern of chromatin solutions at low ionic strength which plays a central role in the model of Bordas et al. (1986b) does not correspond to the "20 nm" feature described by Williams et al. (1986). These authors use a buffer containing 60 mM KCl, 10 mM NaCl (EB-buffer) as well as 3 mM $MgCl_2$ (MB-buffer). Under these conditions chromatin is condensed and the 0.05 nm^{-1} band is no longer visible as also illustrated in Fig. 5. The "20 nm" feature of Williams et al. (1986) corresponds to the band at 0.045 nm^{-1} observed in the patterns of condensed chromatin and also attributed to a subsidiary maximum of the fibre (cylinder) transform by Bordas et al. (1986b).

The available evidence, direct or indirect, thus points to a relationship between linker length and fibre diameter both in condensed chromatin and in uncondensed chromatin at low ionic strength.

Effect of monovalent cations

When $\sqrt{I(0)}$, obtained from $\log(sI(s))$ vs. s^2 plots, is plotted against the number of electrons in the cation $(Z-1)$ at various concentrations of alkali chlorides a set of nearly parallel lines is obtained as illustrated in Fig. 6. The theoretical interpretation of the $\sqrt{I(0)}$ variation in the case of a macroion (DNA) in the presence of various salts (Luzzati et al. 1967) allows one to conclude that at every bulk salt concentration the number of counterions bound to the solute is independent of their nature and that there are no major changes of hydration, as also found for pure DNA. The values obtained by Luzzati et al. (1967) for Li, Na and Cs DNA extrapolated to pure water are also given for comparison in Fig. 6.

Extrapolation of the data in Fig. 6 to $Z=0$ (i.e. the situation in which H^+ is the counterion) yields values which indicate that over the range 0–70 mM

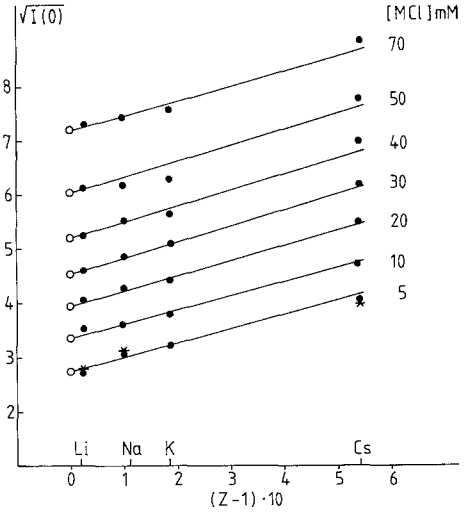

Fig. 6. Plot of $\sqrt{I(0)}$ for CE chromatin solutions (3.5 mg DNA/ml) in the presence of increasing salt (LiCl, NaCl, KCl or CsCl) concentration, against the atomic number of the cation. The asterisks correspond to the values published by Luzzati et al. (1967) for pure DNA

the mass per unit length increases by a factor of up to 8, independent of the nature of the cation.

In the absence of salt the value of $I(0)$ appears to increase again, suggesting that small structural changes occur in those extreme conditions. This is in agreement with the observations of Ausio et al. (1984) who found that at 1 mM NaCl the value of the radius of gyration of the fibres is about 20% higher than at 5 mM NaCl.

The interaction of chicken erythrocyte chromatin with NaCl and divalent cations was recently studied using light scattering and ultracentrifugation (Ausio et al. 1984; Borochov et al. 1984). The chromatin concentrations used for these experiments are about a hundred times lower than in X-ray solution scattering. At high ionic strength (75 mM NaCl) the values of the radius of gyration reported by Ausio et al. (1984) for a chromatin fraction ($A_{260}=0.8$) with 22 nucleosomes is in good agreement with the value obtained by X-ray solution scattering for a fraction ($A_{260}=16.4$) with 23 nucleosomes by Lasters et al. (1985) and consistent with short "30 nm" filaments. Calculations assuming a "10 nm" filament at low ionic strength give values of the radius of gyration which considerably exceed the experimental values and led to the conclusion that the "10 nm" filament is flexible and coils in solution.

Effects of divalent cations and of $Co(NH_3)_6^{3+}$

Although the general features of the condensation induced by divalent cations are similar to the results

previously obtained with $MgCl_2$, there are significant differences between the various cations. In all cases, however, the condensation process, as monitored by the disapperance of the 0.05 nm^{-1} band, is completed before precipitation sets in. Precipitation occurs at chromatin concentrations of 3.5 mg DNA/ml and 2.5 m*M* $MgCl_2$ or about 0.5 Mg^{++}/bp. To a first approximation the mass of the fibre remains unchanged during condensation by divalent cations and $I(0)^{-1}$ is a measure of the relative length of the fibres. As illustrated in Fig. 7, $I(0)^{-1}$ depends linearly on the divalent cation concentration in the range where no precipitation occurs. Cu^{++}, Cd^{++} and $Co(NH_3)_6^{3+}$ induce condensation at lower concentrations than Mg^{++}, $Co(NH_3)_6^{3+}$ being more efficient than any of the divalent cations.

Although in the experiments of Borochov et al. (1984) the onset of precipitation at low chromatin concentrations ($A_{260} = 0.8$) appears to occur at higher Mg^{++}/bp ratios (about 10 Mg^{++}/bp) than in our experiments ($A_{260} = 70$), the trends are very similar.

The relationship between $I(0)$ and the atomic number is much less clear for the divalent than for the monovalent cations. This results from the much smaller concentration range over which the effects can be studied and from the absence of a clear correlation between the atomic number and properties such as the ionic radius and hydration which are likely to influence cation binding. The mass per unit length at a given salt concentration follows the expected sequence for the alkali earth chlorides, $Ba^{++} > Sr^{++} > Mg^{++}$, but Ca^{++} is more efficient in agreement with the results of Staron (1985). The results for Cu and Cd indicate that, as also found by Borochov et al. (1984), the preference of base binding over phosphate binding of metals $Mg^{++} < Co^{++} < Ni^{++} < Mn^{++} < Zn^{++} < Cd^{++} < Cu^{++}$ (Barton and Lippard 1978) also has to be taken into account.

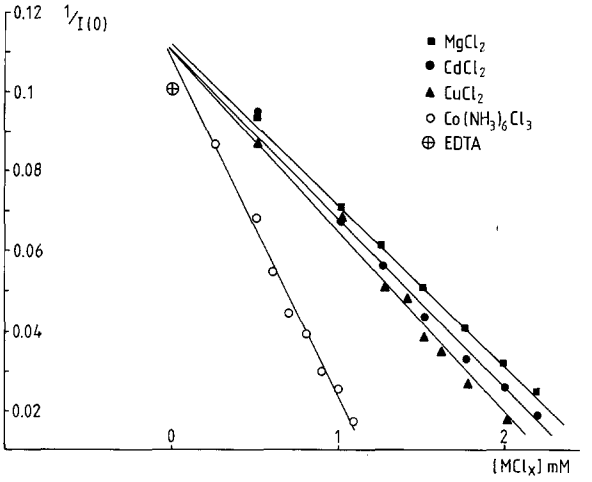

Fig. 7. Change of $I(0)^{-1}$ for CE chromatin solutions (3.5 mg DNA/ml) as a function of concentration of $MgCl_2$, $CuCl_2$, $CdCl_2$ and $Co(NH_3)Cl_6$

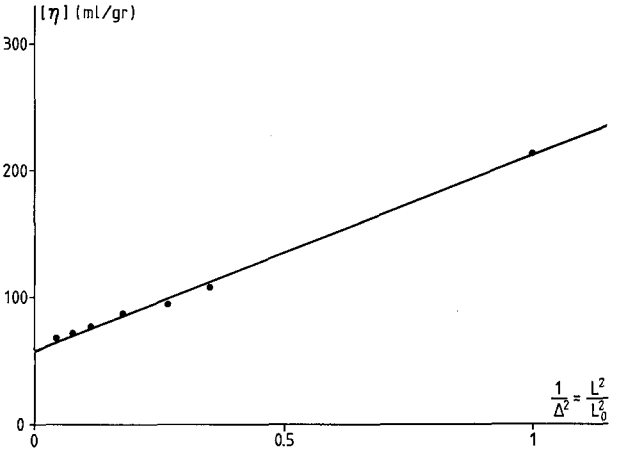

Fig. 8. Relationship between the square of the relative length of the fibre and the intrinsic viscosity for CE chromatin at different Mg^{++}/bp ratios

Comparison between X-ray and hydrodynamic results

The values of the intrinsic viscosity of our chicken erythrocyte chromatin-EDTA preparation obtained by direct measurement or by ultracentrifugation (110 ml/g) is substantially lower than the values reported by Hollandt et al. (1979) for calf thymus chromatin (500–2,400ml/g) but in good agreement with the values recently obtained in the same laboratory for rat liver chromatin (Brust 1985). In contrast, for condensed chromatin (30 ml/g) there is good agreement both with the values of Hollandt et al. (1979) and Brust (1985).

The determination of the mass per unit length and radius of gyration of the cross-section in X-ray solution scattering relies on the assumption that one is dealing with rod-like or worm-like objects. For ideal rods, Kirkwood's equation (see for instance Tanford 1961) gives a relationship between the intrinsic viscosity and the length of the rod. As illustrated in Fig. 8, the relationship between relative length and intrinsic viscosity $[\eta]$ at the same Mg^{++}/bp ratio is consistent with a condensation occurring by reduction of the length of the superstructure at nearly constant diameter. The hydrodynamic studies and calculations of the frictional properties done, however, on the basis of 6 nucleosomes per turn, by Schmitz and Ramsay-Shaw (1977) resulted in an accordion-like model but no unique parameters were obtained.

Comparison with previous X-ray results

Previous X-ray and neutron solution scattering studies on chicken erythrocyte chromatin had led to conclusions quite different from those of Bordas et al. (1986b), at least regarding the low ionic strength structure of chromatin.

Figure 9 illustrates the experimental X-ray solution scattering data published during the last decade. The data obtained since 1979 are all consistent, but differ from those obtained earlier. Since the biochemical characterization is not available, the source of these differences cannot be traced.

Whereas the values of the mass per unit length reported on the basis of those patterns are fairly constant ($2.2-2.9 \cdot 10^5$ Daltons/11 nm), those for the radius of gyration of the cross-section range from 2.5 to 11 nm. As illustrated in curve F in Fig. 9 this results from the particular shape of the scattering curve which makes the determination of the mass per unit length less sensitive to the choice of the region of extrapolation than the radius of gyration of the cross-section. Correct values of both parameters can, however, only be obtained by extrapolation at very low angles (see for instance Porod (1982)). If this is taken into account it is clear that the low ionic strength structure has a diameter of 20–30 nm and that the transition to the so-called 30 nm filament is continuous, as illustrated in Fig. 5.

As stressed earlier by Thoma et al. (1979) and also by Bordas et al. (1986b) the arrangement of nucleosomes both in the lower and higher order structure is irregular. Bordas et al. (1986b) introduced deviations from an ideal structure by averaging the scattering patterns from models with a range of helical parameters. The irregular nature of the structure is confirmed by the recent observations of Widom and Klug (1985) on oriented chromatin where only first order interference bands characteristic of scattering by systems with short range order are observed as opposed to Bragg reflections characteristic of more ordered systems. Recently, Greulich et al. (1986) also emphasized the irregularity of the structure and modelled condensation as a gradual compaction of a wormlike chain. This approach fails, however, to reproduce the 0.05 nm^{-1} band which this group had also observed previously (Reich 1982).

It should be noted that the features of the scattering pattern at low resolution are dominated by the contribution of the nucleosomes, the linker DNA representing only about 20% of the excess scattering mass. Thus, if one neglects the correlation in the orientation of the nucleosomes observed by electric dichroism (McGhee et al. 1980; Mitra et al. 1984), the structure can, to a first approximation, be

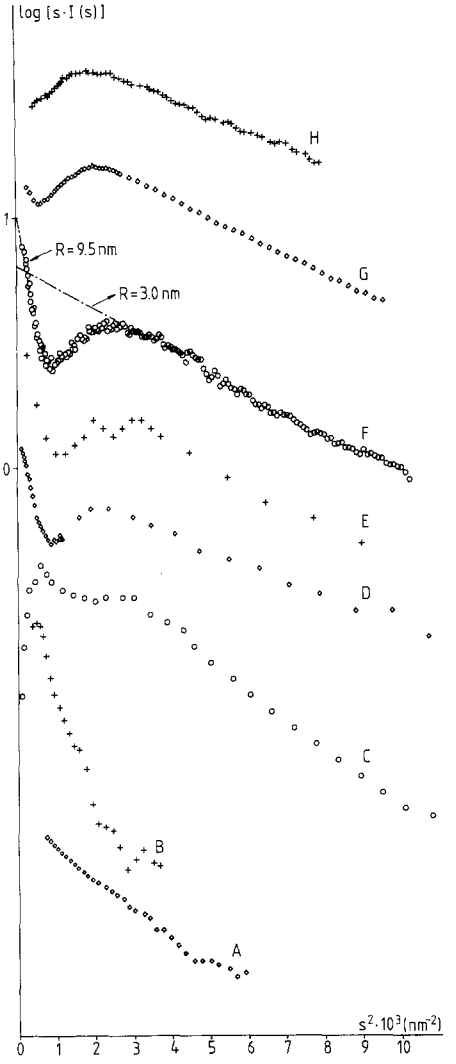

Fig. 9. Chromatin X-ray solution scattering data published since 1976. *A*: Sperling and Tardieu (1976); *B*: Baudy and Bram (1978); *C*: Hollandt et al. (1978); *D*: Suau et al. (1979); *E*: Brust and Harbers (1981); *F*: Perez-Grau et al. (1984); *G*: Notbohm (1986b); *H*: Greulich et al. (1986)

described by the convolution of a wormlike chain and a spherically averaged nucleosome. The scattering pattern is then obtained as the product of the average transform of the wormlike chain and of the nucleosome transform. The results for the average of 100 conformations of a wormlike chain with 70 segments obtained by a Monte Carlo calculation are illustrated in Fig. 10. The length of the segments in the chain was constrained in the range 18–22 nm, the angles between segments were larger than 60° but there were no constraints on the dihedral angles involving three successive segments. The model used for this simple calculation is very reminiscent of the one obtained by electron microscopy by Subirana et al. (1985) for semi-condensed chromatin except that the average internucleosomal distance is only

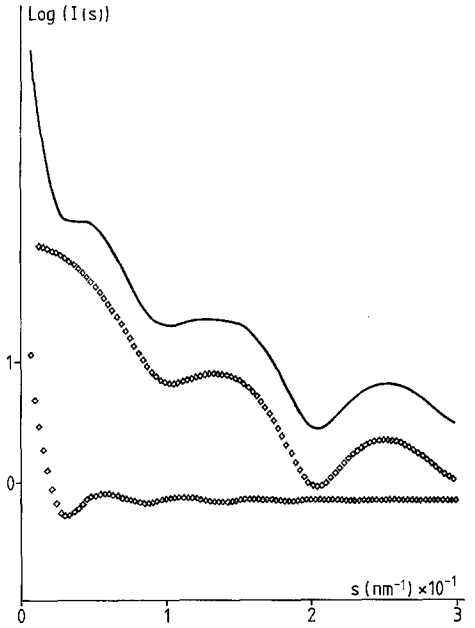

Fig. 10. Theoretical scattering curve (*top*) from a model resulting from the product of the interference of a wormlike chain (*bottom*) and of the transform of a spherically averaged nucleosome (*middle*) illustrating the origin of the 0.05 nm^{-1} band at low ionic strength

about 10 nm in this case. The orientation correlation of the nucleosomes can, however, not be neglected especially at higher condensation levels and at higher resolution. To take this effect into account, the approach of Bordas et al. (1986b) is computationally more efficient.

It should be stressed that some of the models for the structure of chromatin differ essentially only by the path of the linker. In particular, the solenoid model (Finch and Klug 1976) and the crossed linker model of Bordas et al. (1968b) have the same packing density of nucleosomes both at low ionic strength and in the condensed state. As there is, at present, no direct experimental evidence for the path of the linker and the small contribution of the linker to the scattering mass makes it difficult to obtain definitive information by X-ray or neutron scattering, other approaches may be required.

Acknowledgements. We are indebted to Dr. H. Domdey (Laboratory of Molecular Biology, Gene centre, Munich) for kindly providing the initial yeast culture, to Dr. J. Killmartin (MRC Cambridge) for advice on the preparation of yeast nuclei and to Drs. J. Bordas and H. Eisenberg for many useful discussions.

References

Ausio J, Borochov M, Seger D, Eisenberg H (1984) Interaction of chromatin with NaCl and $MgCl_2$. J Mol Biol 177: 373–398

Aviles FJ, Chapman GE, Kneale GG, Crane-Robinson C, Bradbury EM (1978) The conformation of histone H5 isolation and characterization of the globular segment. Eur J Biochem 88:363–371

Axel R, Melchior W, Sollner-Webb B, Felsenfeld G (1974) Specific sites of interaction between histones and DNA in chromatin. Proc Natl Acad Sci USA 71:4101–4105

Barton JK, Lippard J (1978) Heavy metal interaction with nucleic acids. In: Spiro TG (ed) Nucleic acid-metal ions interactions. John Wiley, New York, pp 31–113

Baudy P, Bram S (1978) Chromatin fiber dimensions and nucleosome orientation: A neutron scattering investigation. Nucleic Acids Res 5:3698–3713

Baudy P, Bram S (1979) Neutron scattering on nuclei. Nucleic Acids Res 6:1721–1729

Blodel G, Potter VR (1966) Nuclei from rat liver: Isolation method that combines purity with high yield. Science 154: 1662–1665

Bordas J, Perez-Grau L, Koch MHJ, Nave C, Vega MC (1986a) The superstructure of chromatin and its condensation mechanism. I: Synchrotron radiation X-ray scattering results. Eur J Biophys 13:157–174

Bordas J, Perez-Grau L, Koch MHJ, Nave C, Vega MC (1986b) The superstructure of chromatin and its condensation mechanism. II: Theoretical analysis of the X-ray scattering patterns and model calculations. Eur J Biophys 13: 175–186

Borochov N, Ausio J, Eisenberg H (1984) Interaction and conformational changes of chromatin with divalent ions. Nucleic Acids Res 12:3089–3096

Brandt WF, Patterson K, Holt C von (1980) The histones of yeast: The isolation and partial structure of the core histones. Eur J Biochem 110:67–76

Brust R (1985) Viscosity as an additional physico-chemical parameter for studying chromatin structure. Mol Biol Rep 10:231–235

Brust R, Harbers E (1981) Structural investigations on isolated chromatin of higher-order organisation. Eur J Biochem 117:609–615

Cantor CR, Schimmel PR (1980) Biophysical chemistry Part II: Techniques for the study of biological structure and function. WH Freeman, San Francisco, pp 612–614

Cohen G, Eisenberg H (1968) Deoxyribonucleate solutions: Sedimentation in a density gradient, partial specific volumes, density and refractive index increments, and preferential interactions. Biopolymers 6:1077–1100

Elzinga M, Collins JH, Kuehl WM, Adelstein RS (1973) The complete amino acid sequence of actin of rabbit skeletal muscle. Proc Natl Acad Sci USA 70:2687–2691

Fasman GD (ed) (1976) Handbook of biochemistry and molecular biology, vol 2. CRC Press, Cleveland, Ohio

Finch JT, Klug A (1976) Solenoidal model for superstructure in chromatin. Proc Natl Acad Sci USA 73:1879–1901

Girardet JL, Roche J (1985) Dynamic changes in chromatin superstructure: A light scattering study. Stud Biophys 107: 13–21

Greulich KO, Wachtel E, Ausio J, Seger D, Eisenberg H (1987) Transition of chromatin from the "10 nm" lower order structure, to the "30 nm" higher order structure, as followed by small angle X-ray scattering. J Mol Biol (in press)

Hewish DR, Burgoyne LA (1973) Chromatin sub-structure. The digestion of chromatin DNA at regularly spaced sites by a nuclear deoxyribonuclease. Biochem Biophys Res Commun 52:504–510

Hollandt H, Notbohm H, Riedel F, Harbers E (1979) Studies of the structure of isolated chromatin in three different solvents. Nucleic Acids Res 6:2017–2027

Jenson JC, Chin-Lin P, Gerber-Jenson B, Litman GW (1980) Structurally unique basic protein coextracted with histones from calf thymus chromatin. Proc Natl Acad Sci USA 77: 1389–1393

Johns EW, Phillips DMP, Simson P, Butler JAV (1960) Improved fractionations of arginine-rich histones from calf thymus. Biochem J 77:631–636

Laemmli UK (1970) Cleavage of structural proteins during the assembly of the head of bacteriophage T4. Nature 227: 680–685

Langmore JP, Paulson JR (1983) Low angle X-ray diffraction studies of chromatin structure in vivo and in isolated nuclei and metaphase chromosomes. J Cell Biol 96: 1120–1131

Langmore JP, Schutt C (1980) The higher order structure of chicken erythrocyte chromosomes in vivo. Nature 288: 620–622

Lasters I, Wyns L, Muyldermans S, Baldwin J, Poland GA, Nave C (1985) Scatter analysis of discrete-sized chromatin fragments favours a cylindrical organization. Eur J Biochem 151:283–289

Luzzati V, Masson F, Mathis A, Saludjian P (1967) Etude par diffusion centrale des Rayons X, des polyelectrolytes rigides en solution, cas des sels de Li, Na et Cs du DNA. Biopolymers 5:491–508

Manning GS (1978) The molecular theory of polyelectrolyte solutions with applications to the electrostatic properties of polynucleotides. Q Rev Biophys 11:179–246

McGhee JD, Rau DC, Charney E, Felsenfeld G (1980) Orientation of the nucleosome within the higher order structure of chromatin. Cell 22:87–96

Mitra S, Sen D, Crothers DM (1984) Orientation of nucleosomes and linker DNA in calf thymus chromatin determined by photochemical dichroism. Nature 308:247–250

Notbohm H (1986a) Small angle scattering of cell nuclei. Eur Biophys J 13:367–372

Notbohm H (1986b) Comparative studies on the structure of soluble and insoluble chromatin from chicken erythrocytes. Int J Biol Macromol 8:114–120

Oster G, Riley DP (1952) Scattering from cylindrically symmetric systems. Acta Crystallogr 5:272–276

Pearson EC, Butler PJG, Thomas JO (1983) Higher-order structure of nucleosome oligomers from short repeat chromatin. EMBO J 2:1367–1372

Perez-Grau L, Bordas J, Koch MHJ (1984) Synchrotron radiation X-ray scattering study on solutions and gels. Nucleic Acids Res 12:2987–2995

Porod G (1982) General theory. In: Glatter O, Kratky O (eds) Small angle X-ray scattering. Academic Press, New York, pp 17–53

Rattner JB, Saunders C, Davie JR, Hamkalo BA (1982) Ultrastructural organization of yeast chromatin. J Cell Biol 92: 217–222

Reich M (1982) Small angle X-ray scattering from biological macromolecules. PhD thesis. Weizmann Institute of Science, Rehovot

Renz M, Nehls P, Hozier J (1977) Involvement of histone H1 in the organization of the chromosome fibre. Proc Natl Acad Sci USA 74:1879–1883

Rozijn TH, Tonino GJM (1964) Studies on the yeast nucleus. 1. The isolation of nuclei. Biochim Biophys Acta 91: 105–112

Schmitz KS, Ramsay-Shaw B (1977) Chromatin conformation: A systematic analysis of helical parameters from hydrodynamic data. Biopolymers 16:2619–2633

Sperling L, Tardieu A (1976) The mass per unit length of chromatin by low-angle X-ray scattering. FEBS Lett 64: 89–91

Staron K (1985) Condensation of the chromatin gel by cations. Biochim Biophys Acta 825:289–298

Stratling WH, Muller U, Zentgraf H (1978) The higher order repeat structure of chromatin is built up of globular particles containing eight nucleosomes. Exp Cell Res 117: 301–311

Suau P, Bradbury EM, Baldwin JP (1979) Higher-order structures of chromatin in solution. Eur J Biochem 97:593–602

Subirana JA, Munoz-Guerra S, Aymami J, Radermacher M, Frank J (1985) The layered organization of nucleosomes in 30 nm chromatin fibers. Chromosoma 91:377–390

Tanford C (1961) Physical chemistry of macromolecules. John Wiley, New York

Thoma F, Koller T, Klug A (1979) Involvement of histone H1 in the organization of the nucleosome and of the salt dependent superstructures of chromatin. J Cell Biol 83: 403–427

Thomas JO, Furber V (1976) Yeast chromatin structure. FEBS Lett 66:274–280

Weast RC, Astle MJ (eds) (1979) Handbook of chemistry and physics 59th edn. CRC Press West Palm Beach, USA

Widom J, Klug A (1985) Structure of the 300 Å filament: X-ray diffraction from oriented samples. Cell 43:207–213

Widom J, Finch JT, Thomas JO (1985) Higher-order structure of long repeat chromatin. EMBO J 4:3189–3194

Williams SP, Athey BD, Muglia LJ, Schappe R, Gough AJ, Langmore JP (1986) Chromatin fibres are left-handed double helices with diameter and mass per unit length that depend on linker length. Biophys J 49:233–250

Worcel AS, Strogatz S, Riley D (1981) Structure of chromatin and the linking number of DNA. Proc Natl Acad Sci USA 78:1461–1465

Woodcock CLF, Frado LLY, Rattner JB (1984) The higher order structure of chromatin: evidence for a helical ribbon arrangement. J Cell Biol 99:42–52